

A new pre-conditioned STDP rule and its hardware implementation in neuromorphic crossbar array

Tuomin Tao^a, Da Li^a, Hanzhi Ma^{a,*}, Yan Li^b, Shurun Tan^a, En-xiao Liu^c, Jose Schutt-Aine^d, Er-Ping Li^a

^a Key Laboratory of Advanced Micro/Nano Electronic Devices and Smart Systems and Applications, ZJU-UIUC Institute, Zhejiang University, Hangzhou, China

^b Jiliang University, Hangzhou, China

^c A*STAR Institute of High Performance Computing, Singapore

^d Department of Electrical and Computer Engineering, University of Illinois at Urbana-Champaign, Urbana, USA

ARTICLE INFO

Keywords:

Crossbar array
Memristor
Neuromorphic chips
Spiking neural network
STDP

ABSTRACT

This paper proposes a new pre-conditioned spike-timing-dependent plasticity (STDP) learning rule as well as an efficient system-level time-domain circuit modeling and simulation method for the whole crossbar array structure. First, the new pre-conditioned STDP rule is conceived by exercising a slight perturbation to the conventional STDP curve. Software-wise, it can be described in spiking neural network (SNN) codes, while hardware-wise, it is realized by the memristor crossbar array in conjunction with specific spike signals, just as the conventional STDP. The new STDP rule enables the neural network in a neuromorphic chip to achieve better performance both in terms of software and hardware implementation compared with the conventional STDP rule. Second, a time-domain circuit modeling method is proposed for the simulation of the whole crossbar array. Numerical experiments demonstrate that the new pre-conditioned STDP is superior to the conventional STDP both in terms of accuracy and low power consumption. At the software level, a 784×100 spiking neural network, trained by the pre-conditioned STDP, for the MNIST handwritten digit recognition achieves an accuracy of 85.90%, which is 3.09% higher than that trained by the conventional STDP. At the hardware level, a down-scaled 196×10 crossbar array is simulated and trained. The crossbar array trained by the new STDP consumes 21.5% less power than that trained by the conventional STDP. Moreover, it does not compromise the original robustness when subject to non-ideal characteristics such as variation of conductance and resistance of the interconnect in the crossbar array.

1. Introduction

PIKING neural network (SNN) is the third-generation neural network model whose input and output information is encoded by spike sequences [1,2]. It imitates the characteristics of the human brain neural network more closely than the second-generation neural network that relies on activation functions and gradient decent algorithms. The event-driven spiking neural network has been proved suitable for implementation in neuromorphic computing chips to achieve energy-efficient machine intelligence [3–5].

Different kinds of supervised [6–9] and unsupervised [10–13] SNN algorithms have been developed, where the unsupervised learning rule based on spike-timing-dependent plasticity (STDP) is of great interest,

which is a biological characteristic of the synapses connecting different neurons. The working mechanism of the biological neurons is shown in Fig. 1(a). The neurons connect with each other by the synapses, whose connection strength is adjusted by the arriving time difference between the pre- and post-synaptic spikes, as shown in Fig. 1(b). This special rule makes the spiking neural network capable of learning. Emerging memristors [14,15] are believed to be excellent artificial synapses. A memristor is a two-electrode device and its conductive filament can grow or decrease with the voltage across the memristor [15]. The characteristic of the adjustable conductance is similar to the synaptic weight. With the ability to conduct fast vector-matrix multiplications and the tunability in conductance, the memristor crossbar array, a key building block in non-von Neumann neuromorphic chip, enables fast in-memory

* Corresponding author at: Key Laboratory of Advanced Micro/Nano Electronic Devices and Smart Systems and Applications, ZJU-UIUC Institute, Zhejiang University, Hangzhou, China.

E-mail address: mahanzhi@zju.edu.cn (H. Ma).

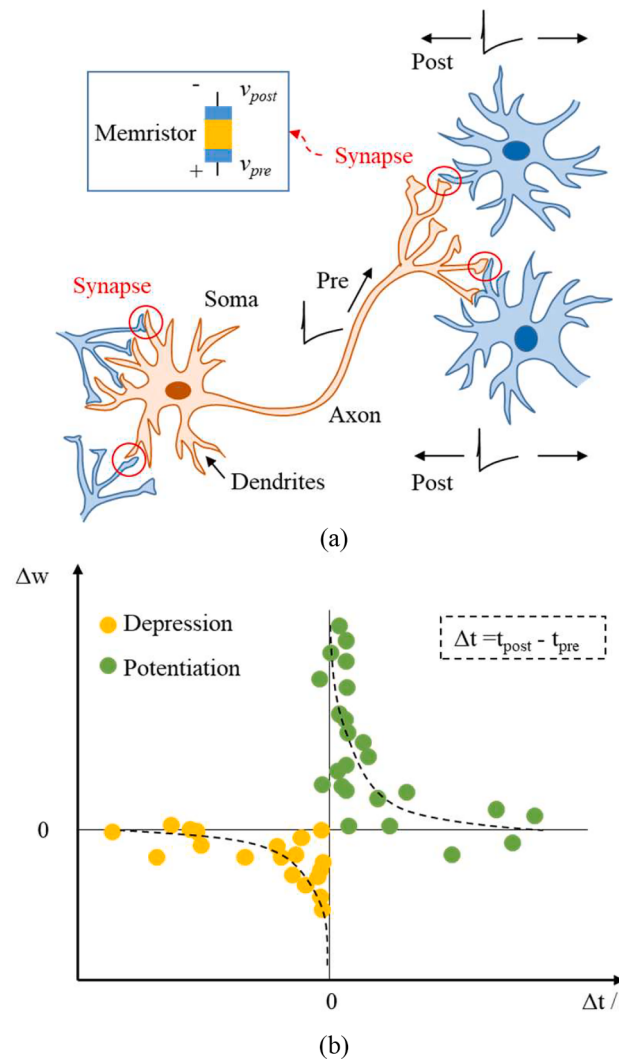


Fig. 1. Biological neural network. (a) Diagram of typical biological neurons. (b) Biological STDP rule of synapses.

calculation [16,17] with better efficiency and lower power consumption than the traditional semiconductor device based chip.

Many researchers have investigated the topic of learning with unsupervised STDP rules based on memristor crossbar array. Both experimental and theoretical approaches are studied in [18] to search for effective local training rules to achieve unsupervised pattern recognition by memristor-based Spiking Neural Networks. The applicability of temporal encoding to training spiking networks with memristor-based STDP is illustrated in [19]. A novel memristive synapse model is proposed in [20] by using HP memristors. However, these works haven't involved any circuit modeling and simulation of the whole memristor crossbar array. A set of piecewise linear approximations of STDP rules is presented in [21]. STDP rules with different shapes which can be implemented by different spike signals are compared in [22]. However, in both cases the performance of the proposed STDP rules has not been proved in neuromorphic chips. An STDP rule realized by the HfO₂ memristor device and its corresponding compact model are proposed in [23]. A simplified STDP rule is proposed in [24] to make the neuromorphic crossbar array immune to device variations. Nevertheless in both studies the pre- and post-synaptic signals by such STDP rule are square wave signals rather than biological nerve spike signals. The STDP rule in [25] implemented by the memristor and the spike signal can emulate the simplest associate learning of a Pavlov's dog. But the size of its spiking neural network is extremely small with only three neurons

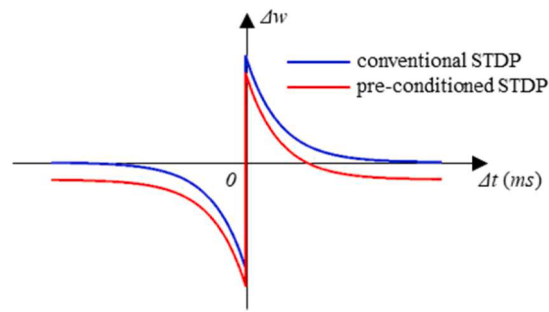


Fig. 2. The conventional STDP rule and the new pre-conditioned STDP rule.

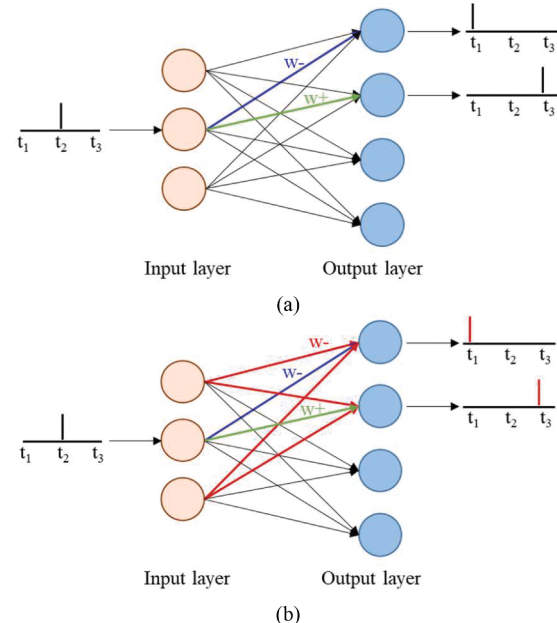


Fig. 3. A two-layer spiking neural network based on (a) the conventional STDP rule in the neural network and (b) the new pre-conditioned STDP rule.

and two synapses.

In this paper, a new pre-conditioned STDP rule is proposed, which provides better performance both in software and neuromorphic crossbar array implementation compared with the conventional STDP rule. At the software level, the new STDP rule achieves higher recognition accuracy for the Mixed National Institute of Standards and Technology (MNIST) [26] handwritten digit classification. Furthermore, this paper also presents a time-domain circuit simulation method for crossbar SNN training. At the hardware level, the neuromorphic crossbar array trained by the new pre-conditioned STDP rule consumes less power and shows better robustness.

The rest of this paper is organized as follows: Section II introduces the new pre-conditioned STDP rule and its performance in SNN in contrast with the conventional STDP rule. Section III illustrates the implementation method of the two STDP rules in crossbar array. The circuit modeling of the whole crossbar array structured is also presented. Section IV shows the performance of the two STDP rules in the circuit training of SNN. The conclusion is presented in Section V.

2. The pre-conditioned STDP and its performance in SNN

2.1. The pre-conditioned STDP

The conventional STDP rule fitting with Fig. 1(b) is described by [22]:

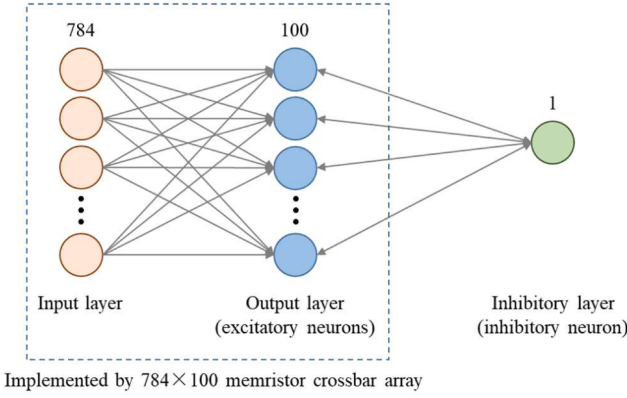


Fig. 4. The three-layer spiking neural network.

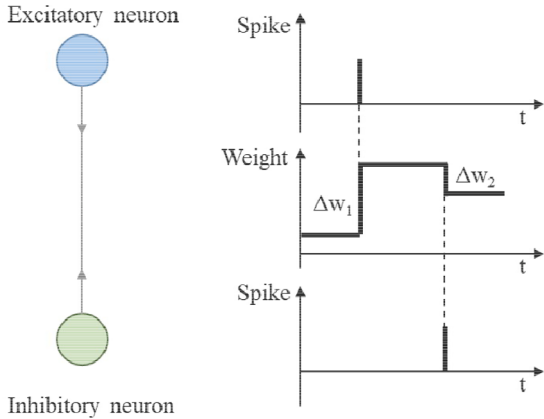


Fig. 5. Lateral inhibition and homeostasis.

$$\Delta w(\Delta t) = \begin{cases} A_{pre} e^{-\Delta t/\tau_{pre}} \Delta t > 0, \\ A_{post} e^{\Delta t/\tau_{post}} \Delta t < 0, \end{cases} \quad (1)$$

where Δt is the time difference between the pre- and post-synaptic spikes and Δw is the value of the weight changed by the two spikes. The conventional STDP rule is shown in Fig. 2. By exercising a slight perturbation to the conventional STDP curve, a pre-conditioned STDP rule is obtained as:

$$\Delta w(\Delta t) = \begin{cases} A_{pre} e^{-\Delta t/\tau_{pre}} - k \Delta t > 0 \\ A_{post} e^{\Delta t/\tau_{post}} - k \Delta t < 0 \end{cases} \quad (2)$$

The distinctive advantage of the pre-conditioned STDP rule is evident by comparing Fig. 3(a) and (b), which shows the conventional and the pre-conditioned STDP adjustment in a two-layer spiking neural network. The new STDP is able to adjust the weights of those synapses rarely receiving pre-synaptic spikes (see the red lines marked with w - in Fig. 3(b)). This characteristic leads to better training results of the spiking neural network, as will be demonstrated in the next subsection.

2.2. Performance of the pre-conditioned STDP in SNN

A three-layer spiking neural network is designed based on the pre-conditioned STDP rules, as shown in Fig. 4. The network is simulated by Python and the Brian simulator [27]. It is applied to classify handwritten digits of the MNIST dataset. The input layer contains 784 neurons corresponding to the 28×28 pixels of one image. The output layer contains 100 excitatory neurons. The training results will be better if more output neurons are adopted, while the computational complexity will increase as well.

Lateral inhibition is a biological phenomenon in which the firing

Table 1
Parameter Values of Neurons.

Parameter	Excitatory neuron	Inhibitory neuron
E_{rest}	-65 mV	-60 mV
E_{exc}	0 mV	0 mV
E_{inh}	-100 mV	-85 mV
τ	100 ms	10 ms
v_{reset}	-65 mV	-45 mV

neuron inhibits all other neurons. This mechanism leads to competition among excitatory synapses and causes them to have different firing rates. However, it is desirable that all neurons have approximately equal firing rates to prevent single neuron from dominating the learning process and to ensure that each neuron learns a different pattern. So homeostasis should also be considered to balance the firing rate. In this work, the lateral inhibition and homeostasis is implemented by simplifying the method proposed in [28]: One inhibitory neuron connects with all the excitatory neurons of the output layer, as shown in Fig. 4. The weight variation programmed by the transmitted spikes is described in Fig. 5. When the excitatory neuron spikes, the corresponding synaptic weight increases by Δw_1 . The excitatory spike also causes the inhibitory neuron to fire because the threshold membrane voltage of the inhibitory neuron is very low. All of the synaptic weights decrease by Δw_2 due to the inhibitory spike. Assuming that

$$\Delta w_1 = p \times \Delta w_2 \quad (3)$$

p is roughly equal to the number of excitatory neurons, which is set as 100 in this work. One spike from excitatory neuron is enough to excite the inhibitory neuron since the threshold of the inhibitory neuron is set to be low. Under this mechanism, if one excitatory neuron spikes too frequently, the connected inhibitory synaptic weight will increase significantly so that the spike frequency will decrease due to high inhibitory intensity. Similarly, if one excitatory neuron hardly spikes, the inhibitory weight will keep decreasing to help the neuron get more chance to fire.

The leaky integrated-and-fire model [11] is chosen to model the neuron. The membrane voltage V is described as:

$$\tau \frac{dV}{dt} = (E_{rest} - V) + g_e(E_{exc} - V) + g_i(E_{inh} - V), \quad (4)$$

where E_{rest} is the resting membrane potential, E_{exc} and E_{inh} are the equilibrium potentials of excitatory and inhibitory synapses, g_e and g_i are the conductances of excitatory and inhibitory neurons, and τ is a time constant. The neuron fires when the membrane voltage exceeds the threshold and it cannot fire again in its refractory period, during which the membrane voltage is reset to v_{reset} .

The input spike sequences are encoded from handwritten digit pictures of the MNIST dataset. Each picture contains 784 pixels with the pixel intensity from 0 to 255. Each pixel is encoded as a 500 ms spike train. The first 350 ms of them conform to Poisson distribution, whose firing rates are a quarter of the corresponding pixel intensity. So the firing rates are in the range of 0 to 63.75 Hz. Besides, there are no inputs in the remaining 150 ms so that all the neurons will decay to the resting state.

To train the network, the 60,000 training examples from the MNIST dataset are presented to the network for three times. So the training

Table 2
Parameter Values of STDP.

Parameter	New_STDP	Conv_STDP
A_{pre}	0.00123	0.001196
A_{post}	-0.00048	-0.00048
τ_{pre}	20 ms	20 ms
τ_{post}	25 ms	25 ms
k	-0.00001	-

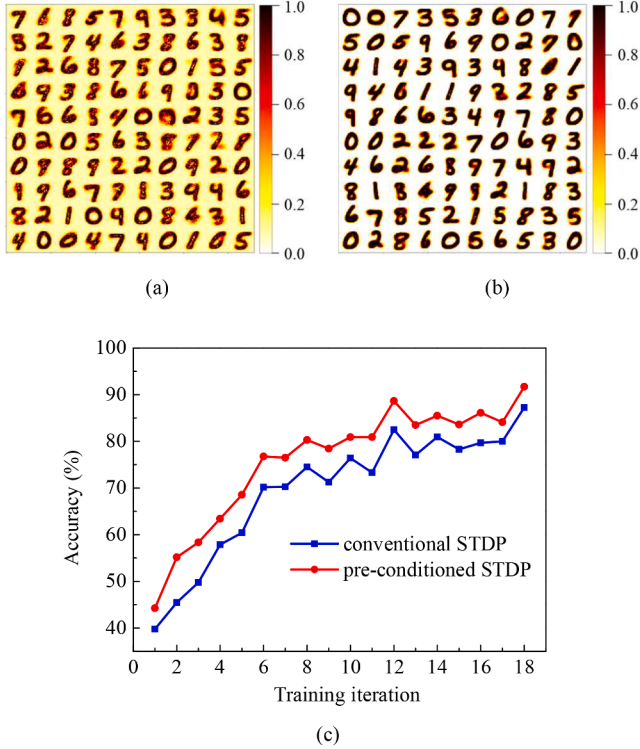


Fig. 6. Training results. (a) Rearranged weights trained by the conventional STDP rule. (b) Rearranged weights trained by the proposed STDP rule. (c) Recognition accuracy of the two training cases after every 10,000 training examples.

process contains 180,000 sets of input spike trains. The weights between the input and the output layer are limited in the range from 0.01 to 1 and the initial values of weights are normally distributed around 0.08. For comparison, another network with same structure based on the conventional STDP rule is also trained besides the network based on the pre-conditioned STDP rule. The parameter values of the neurons and STDP of the spiking neural network are listed in Table 1 and Table 2, respectively.

The rearranged weights of the two training cases are shown in Fig. 6 (a) and (b). For each output neuron, the 784 connected synaptic weights are rearranged into a 28×28 matrix to visualize the prototypical digit

the neuron learns. A clearer pattern is generated when it is learned by the pre-conditioned STDP. Moreover, the pre-conditioned STDP can decrease the synaptic weights to minimum for synapses rarely receiving input signals. Such a feature further enhances the quality of the learned patterns. The 180,000 training sets are divided into 18 training iterations. The last 2000 training examples of each iteration are used for labeling the output neurons so that the recognition accuracy of this iteration can be calculated. The accuracy of the two cases is compared in Fig. 6(c). The pre-conditioned STDP rule consistently performs better than the conventional STDP rule. In addition, if we use 10,000 testing samples after the training process, the final accuracy achieved by the pre-conditioned and the conventional STDP is 85.90% and 82.81%, respectively. Result comparisons with other SNNs based on STDP for MNIST classification are listed in Table 3. The accuracy of the proposed training method can be further improved by increasing the output

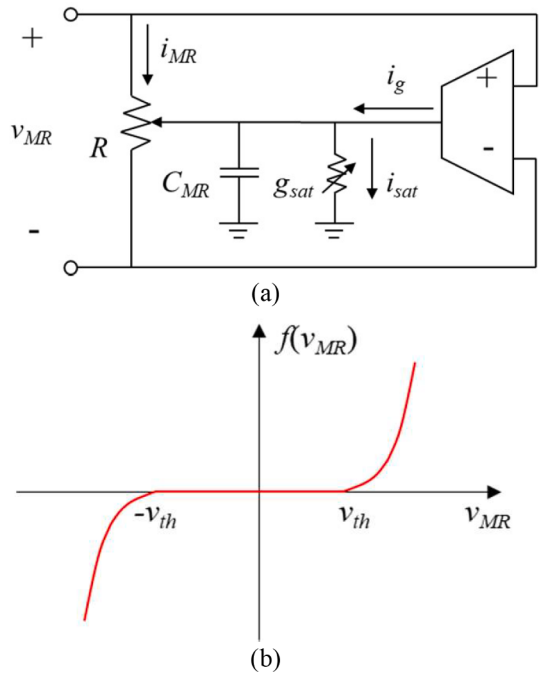


Fig. 7. (a) Macro-model circuit of the memristor. (b) Memristor non-linear weight update function.

Table 3
Comparisons with Other SNNs Based on STDP for MNIST Classification.

	Device	Learning rule	Lateral inhibition	Homeostasis	Output neurons	Performance
Diehl's work [11]	None	Exponential STDP	Inhibitory neurons as many as excitatory neurons	Membrane threshold changes according to variable θ	100 400 600 6400	82.9% 87.0% 91.9% 95.0%
Demin's work [18]	$(\text{CoFeB})_x(\text{LiNbO}_3)_{1-x}$ memristive device	Exponential STDP	Winner-take-all	weight decay potentially takes place at each post-synaptic spike	25 50 100	65.78% 78.55% 89.15% (for cropped images)
Querlioz's work [24]	Memristive device	Rectangular STDP	Winner-take-all	Membrane threshold changes according to a target activity	50 300	81% 93.5%
Hansen's work [29]	$\text{Al}/\text{Al}_2\text{O}_3/\text{Nb}_x\text{O}_y/\text{Au}$ memristive device	Rectangular STDP	Winner-take-all	Membrane threshold changes according to a target activity	10 20 50 100	65% 70% 77% 82%
Guo's work [30]	Resistive random access memory (RRAM)	Exponential STDP	Winner-take-all	Membrane threshold changes according to a target activity	50	78.9%
This work	Memristive device	Pre-conditioned exponential STDP	One inhibitory neuron	One inhibitory neuron	100	85.90%

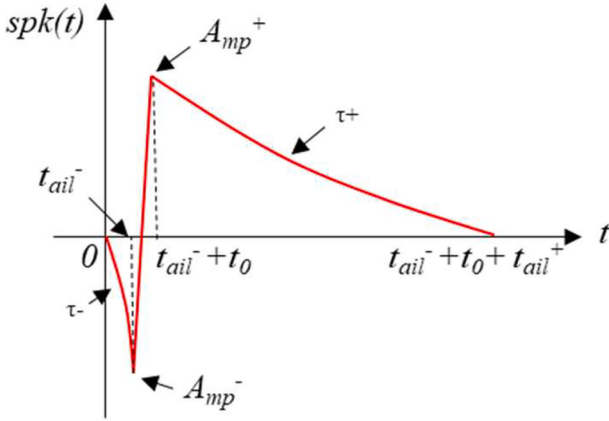


Fig. 8. The spike waveform.

neurons. The scaling method contains two steps: the first step is to adjust the connection parameter p between the output and the inhibitory layer, the second step is to adjust the hyper-parameters of STDP, especially A_{pre} and A_{post} .

3. STDP implementation in neuromorphic crossbar array

3.1. The memristor and the spike model

Both conventional and pre-conditioned STDP rules are realized by memristors and spike signals. The macro-model of the memristor proposed in [31] is adopted for circuit simulation in this work, as represented in Fig. 7(a). The ionic drift under electric fields in the memristor is defined as:

$$f(v_{MR}) = \begin{cases} I_0 [e^{v_{MR}/v_o^+} - e^{v_{th}^+/v_o^+}] & v_{MR} > v_{th}^+ \\ -I_0 [e^{-v_{MR}/v_o^-} - e^{-v_{th}^-/v_o^-}] & v_{MR} < v_{th}^- \\ 0 & \text{otherwise} \end{cases}, \quad (5)$$

where v_{MR} denotes the voltage across the memristor. v_{th}^+ and v_{th}^- denotes the positive and negative thresholds of the memristor. v_o^+ and v_o^- are used to fit the performance of the memristor. The function of the memristor model is drawn in Fig. 7(b). In this work, the memristor model doesn't consider the hysteresis property and their initial conductivity is independent on the synaptic change of weight. The simplification of the model aims to enable the memristor to achieve approximate STDP curves with relatively less computational complexity during the time-domain circuit simulation of crossbar array.

The memristor is able to realize STDP rules under the influence of particular pre- and post- synaptic spikes. The spike function in [22] is modified so that it can be used for circuit simulation in time domain:

$$spk(t) = \begin{cases} A_{mp}^- e^{(t-t_{ail}^-)/\tau^-} - e^{-t_{ail}^-/\tau^-} & 0 < t \leq t_{ail}^- \\ A_{mp}^- + \frac{(A_{mp}^+ - A_{mp}^-) \times (t - t_{ail}^-)}{t_0} & t_{ail}^- < t \leq t_{ail}^- + t_0 \\ A_{mp}^+ e^{-(t-t_{ail}^- - t_0)/\tau^+} - e^{-t_{ail}^+/\tau^+} & t_{ail}^- + t_0 < t \leq t_{ail}^- + t_0 + t_{ail}^+ \\ 0 & \text{otherwise} \end{cases}. \quad (6)$$

The spike waveform and its parameters are shown in Fig. 8. Therefore, the voltage across the memristor is described by:

$$v_{MR}(t, \Delta t) = spk(t) - spk(t + \Delta t). \quad (7)$$

Based on Eq. (5) and Eq. (6), the synaptic weight update can be

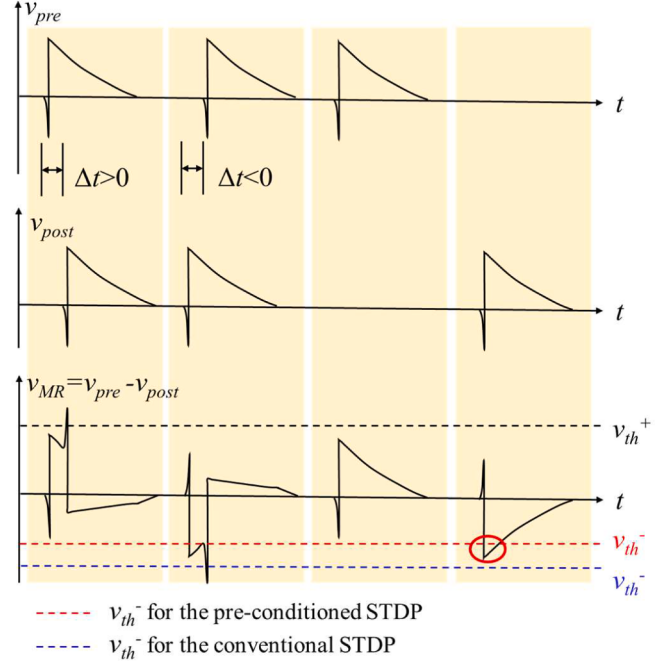


Fig. 9. (a) The realization of the conventional and the pre-conditioned STDP rule based on the memristor and the spike. (b) The conventional and the pre-conditioned STDP curves realized by the memristor and the spike.

obtained by the following integral:

$$\Delta w(\Delta t) = \int f(v_{MR}(t\Delta t)) dt \quad (8)$$

which has the same shape as the STDP curve in consistence with Eq. (1).

Fig. 9(a) illustrates the realization of the conventional and the pre-conditioned STDP rule based on the memristor and the spike. V_{pre} and V_{post} (see Fig. 1(a)) represent the pre- and post-synaptic voltage, respectively. When the voltage across the memristor exceeds the positive/negative threshold v_{th}^+ and v_{th}^- , the conductance of the memristor will increase/decrease. The positive voltage thresholds of the two cases are the same but the negative thresholds are different. The thresholds should satisfy the following inequalities:

$$A_{mp}^+ < v_{th}^+ < A_{mp}^+ - A_{mp}^- \quad (9)$$

$$A_{mp}^- - A_{mp}^+ < v_{th(conv.)}^- < -A_{mp}^+ < v_{th(modif.)}^- < A_{mp}^- \quad (10)$$

In the conventional STDP case, the conductance changes only when the memristor receives both pre- and post- spikes within a certain time frame, but the conductance in the pre-conditioned STDP case can be adjusted even when a post-synaptic spike is received alone. Besides, if a pre-synaptic spike is received in the absence of a post-synaptic spike, the conductance in both cases will not change. The conventional and the

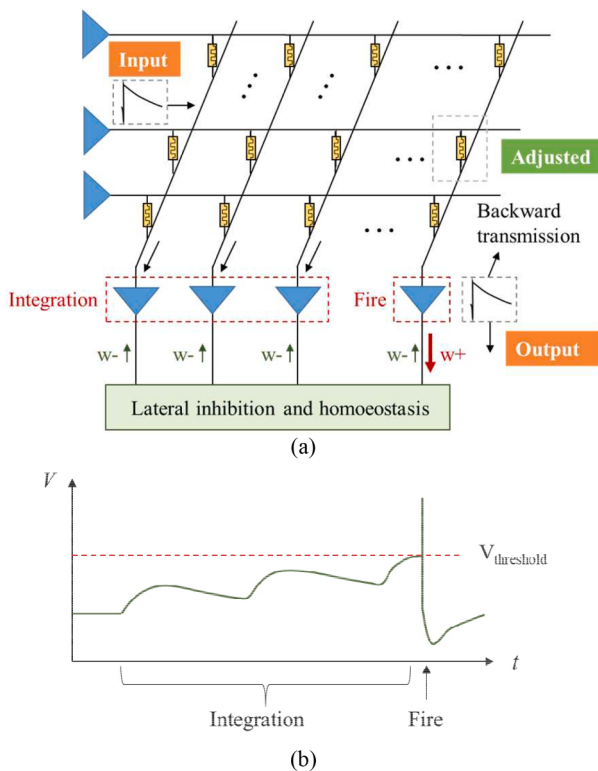


Fig. 10. (a) Neuromorphic memristor crossbar array. (b) The leaky integrated-and-fire model.

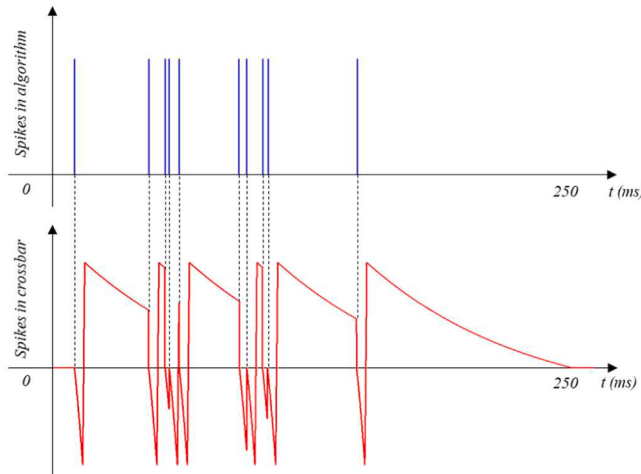


Fig. 11. The spike waveform in SNN algorithm and crossbar array.

pre-conditioned STDP curves realized by the two memristors of different negative thresholds with the same spike signal are shown in Fig. 9(b).

3.2. Circuit modeling of the crossbar array

The working mechanism of the neuromorphic memristor crossbar array is described in Fig. 10(a). The output neurons have two states: integration and firing, as shown in Fig. 10(b). At the integration state, they receive and integrate the input current signals, while at the firing state, they generate both the output and backward-transmission spikes at the same time. The input pre-synaptic spike and the backward-transmission post-synaptic spike can adjust the conductance of the corresponding memristor. What's more, the lateral and homeostasis mechanism changes the spike frequencies of the output neurons

according to the output spikes.

The input spike sequences only contain the information of the spike time in the SNN algorithm trained in Section II. However, when it is trained on the crossbar array, the input spike sequences have specific waveforms. One pixel is usually encoded as a spike sequence lasting for hundreds of milliseconds, while one spike signal may also last for tens or even hundreds of milliseconds. So the overlap between spike signals is inevitable in the crossbar array. In this work, the next spike signal will overwrite the previous one in the input spike sequence, as shown in Fig. 11.

The synaptic weights are distributed from 0.01 to 1 in the SNN algorithm introduced in Section II. In circuit simulation, the high resistance state (HRS) and low resistance state (LRS) of the memristor is assumed to be $100\text{ k}\Omega$ and $1\text{ k}\Omega$. And the initial synaptic weights can be linearly mapped to the memristor conductance. In other words, the initial synaptic weights w is inversely proportional to the memristor resistance R as follows:

$$R = \frac{1}{w}k\Omega \quad 0.01 \leq w \leq 1 \quad (11)$$

The circuit simulation of the SNN training on the crossbar array is conducted in MATLAB [32]. The neurons as well as the lateral and homeostasis mechanism are described by behavioral models. The method of the circuit simulation of the crossbar array in time domain has been introduced in the previous work [17]. Here, the circuit model of the crossbar array can be obtained by the domain decomposition method (DDM) and the partial equivalent element circuit (PEEC) method. The time-domain circuit simulation is then described by matrix function:

$$\begin{bmatrix} -A & -\left(R + L \frac{d}{dt}\right) \\ C \frac{d}{dt} & -A^T \end{bmatrix} \begin{bmatrix} V \\ I \end{bmatrix} = \begin{bmatrix} V_s \\ \mathbf{0} \end{bmatrix} \quad (12)$$

where R , L , C represents the resistance, inductance, and short circuit capacitance matrix, A represents the connectivity matrix, V_s is the voltage source excitation. V and I are node voltages and branch currents to be solved. Since the duration of the spike signal lasts for milliseconds and the size of the crossbar array is relatively small, the influence of the parasitic inductance and capacitance is negligible in such low frequency situation. In this way, the matrix function is simplified as:

$$\begin{bmatrix} -A & -R \\ \mathbf{0} & -A^T \end{bmatrix} \begin{bmatrix} V \\ I \end{bmatrix} = \begin{bmatrix} V_s \\ \mathbf{0} \end{bmatrix} \quad (13)$$

To reduce the computational complexity and simulation time, only three representative handwritten digits “0”, “1”, “7” are classified in the circuit training of SNN as many computer vision algorithms tend to distinguish “1” and “7” poorly. Moreover, the 784 pixels per image is down-sampled to 196 pixels per image and the output neurons are decreased from 100 to 10. Thus, the size of the crossbar array is reduced from 784×100 to 196×10 . Each pixel is encoded as a 300 ms spike

Table 4
Parameter Values of Memristor and Spike Model.

	Parameter	Value (new_STDP)	Value (conv_STDP)
Memristor	v_{th}^+	1 V	
	v_{th}^-	-0.92 V	-1 V
	v_0^+	0.83 V	0.88 V
	v_0^-	1.50 V	
	I_0	0.2 A	
	A_{mp}^+	1 V	
	A_{mp}^-	-0.92 V	
	τ^+	80 ms	
	τ^-	10 ms	
	t_{ail}^+	100 ms	
Spike	t_{ail}^-	4 ms	
	t_0	1 ms	

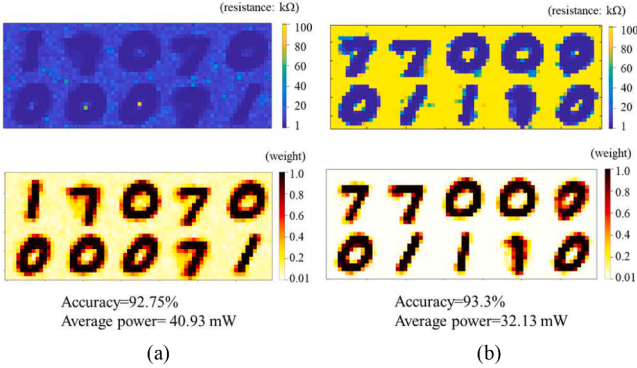


Fig. 12. (a) The memristor resistance and weight distributions trained by the conventional STDP and (b) the pre-conditioned STDP.

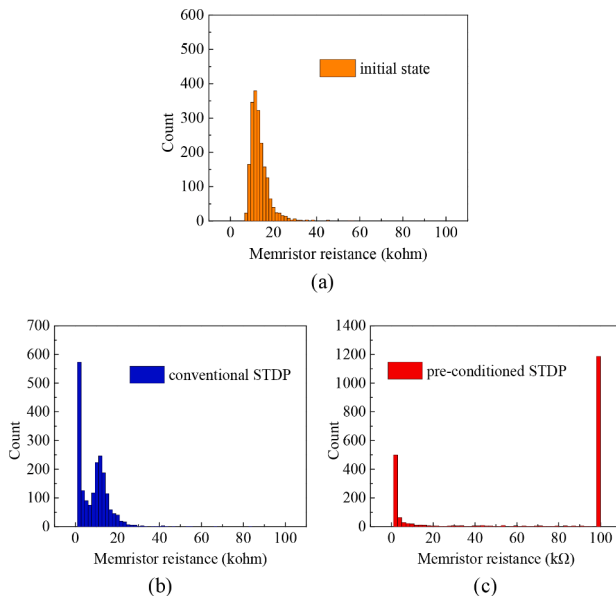


Fig. 13. The numerical statistics of the memristor resistance (a) at initial state, (b) after training of the conventional STDP and (c) after training of the pre-conditioned STDP.

train. The first 150 ms of them conform to Poisson distribution whose firing rates are a quarter of the corresponding pixel intensity and the remaining 150 ms contains no inputs.

4. Performance of the pre-conditioned STDP in neuromorphic crossbar array

4.1. Performance comparisons of the two STDP rules

The parameters of the memristor and spike model are adjusted to realize the pre-conditioned STDP and achieve a high recognition accuracy. For comparison, the parameters of the memristor are adjusted again to realize the conventional STDP with the same spike model. The parameters of the two cases are listed in Table 4. The listed parameters of the memristor and the spike correspond with the parameters in Eq. (5) and Eq. (6). The rearranged memristor resistance after training of the two cases and their corresponding weight distributions are shown in Fig. 12 (a) and (b). For each output neuron, the 196 connected memristors are rearranged into a 14×14 matrix to visualize the prototypical digit the neuron learns. The conventional and the pre-conditioned STDP achieve recognition accuracies of 92.75% and 93.3%, respectively. The advantage of the pre-conditioned STDP is small because the

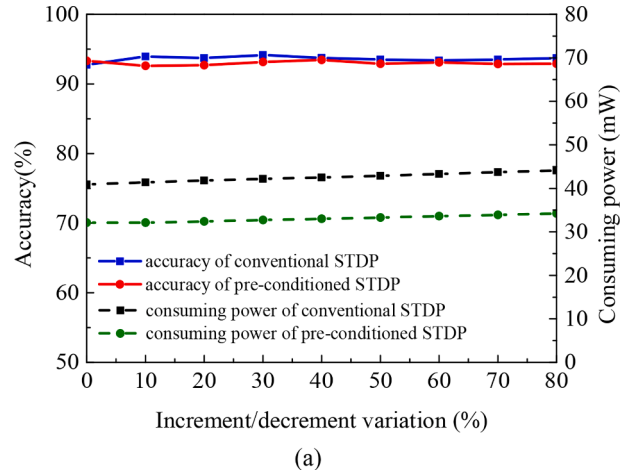


Fig. 14. (a) The influence of the conductance increment/decrement variation. (b) The influence of the conductance increment/decrement and Gmin/Gmax variation.

classification task is quite simple. The average power of the training process by the pre-conditioned STDP is 32.13 mW, which is 21.5% less than 40.93 mW consumed by the conventional STDP.

The advantage of less consuming power lies in the resistance distribution of the crossbar array. The numerical statistics of the memristor resistance at initial state and after training of the conventional and pre-conditioned STDP are presented in Fig. 13. A large number of the memristors trained by the pre-conditioned STDP are at high resistance state which leads to lower power consumption.

4.2. Influence of non-ideal characteristics

The non-ideal characteristics of the memristor as well as the interconnect are incorporated into the circuit simulation of SNN to compare the robustness and power consumption of the two STDP cases.

Firstly, the conductance increment/decrement variation of the 1960 memristors is added. The variation is defined by relative standard dispersion (the ratio between variation and mean value of the parameter). The accuracy and consuming power of the two cases are illustrated in Fig. 14 (a). The accuracies of both cases are similar and almost unchanged. The robustness of the conventional STDP is slightly better, but the consuming power of the pre-conditioned STDP is always lower than that of the conventional STDP.

Then, we introduce the variation of maximum and minimum conductance on the basis of the increment/decrement variation, as shown in Fig. 14 (b). When the variation is less than 50%, the results are

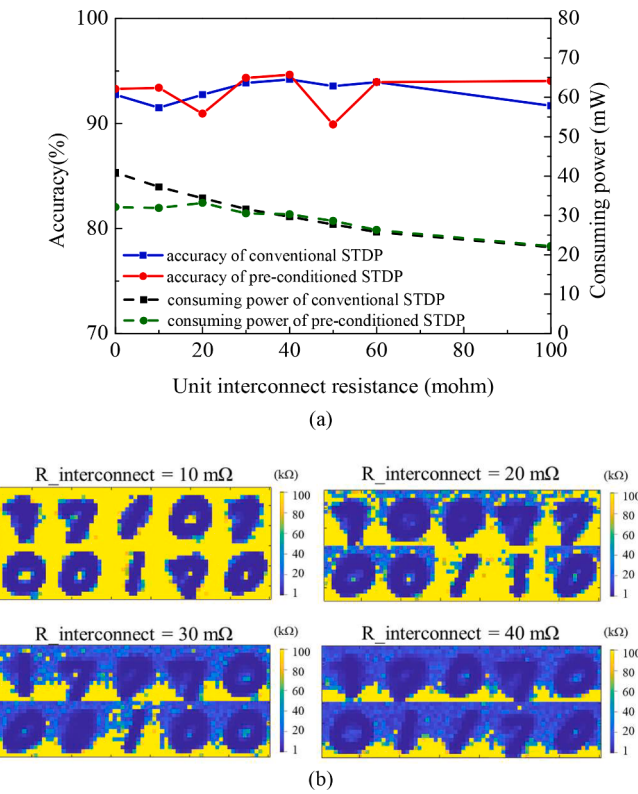


Fig. 15. (a) The influence of the unit interconnect resistance. (b) The memristor resistance distribution with different interconnect resistance trained by the pre-conditioned STDP.

similar to the case with only increment/decrement variation in which the conventional STDP achieves better robustness but consumes more power. When the variation is more than 50%, the accuracy of the conventional STDP drops faster.

Finally, the interconnect resistance of the crossbar array is considered. The interconnect resistance can lead to IR-drop and sneak-path problems which may influence the training results of SNN. Fig. 15 (a) describes the influence of the unit interconnect resistance on the accuracy and consuming power. The influence of the interconnect resistance on the accuracy is quite random. SNN has the ability to make up for the small non-ideal factors and can even achieve better recognition accuracy. Overall, the accuracy of the pre-conditioned case changes more dramatically. As for the power consumption, when the interconnect resistance is less than 40 mΩ, the consuming power of the pre-conditioned STDP is lower. However, the advantage in consuming power of the pre-conditioned STDP disappears. This phenomenon is mainly caused by the IR drop on the interconnect resistance. Fig. 15 (b) shows the change process of the memristor resistance distribution when the unit interconnect resistance changes from 10 mΩ to 40 mΩ. As the interconnect resistance increases, the voltage across the memristor is no longer able to decrease the conductance when the post-synaptic neuron spikes alone.

5. Conclusion

This paper presents a pre-conditioned STDP rule that is conceived by exercising a slight perturbation to the conventional STDP curve. The pre-conditioned STDP rule can be described in algorithm codes and realized on the memristor crossbar array by using particular spike signals. It achieves better performance over the conventional STDP rule both in the software and hardware level.

At the software level, due to more effective weight adjustment, the spiking neural network trained by the pre-conditioned STDP achieves a

recognition accuracy of 85.90%, which is 3.09% higher than the network trained by the conventional STDP.

At the hardware level, this paper proposes a time-domain circuit simulation method for the crossbar array to train a spiking neural network. Based on the simulation results, the crossbar array trained by the pre-conditioned STDP consumes 21.5% less power than that trained by the conventional STDP, since the former has a larger number of memristors with high resistance. Moreover, the crossbar array trained by the pre-conditioned STDP does not compromise the original robustness when non-ideal characteristics such as conductance increment/decrement variation, maximum/minimum conductance variation and interconnect resistance are employed to the crossbar array.

CRediT authorship contribution statement

Tuomin Tao: Conceptualization, Methodology, Software, Formal analysis, Writing – original draft. **Da Li:** Validation, Writing – review & editing. **Hanzhi Ma:** Supervision, Writing – review & editing. **Yan Li:** Writing – review & editing. **Shurun Tan:** Writing – review & editing. **En-xiao Liu:** Writing – review & editing. **Jose Schutt-Aine:** Writing – review & editing. **Er-Ping Li:** Supervision, Writing – review & editing.

Declaration of Competing Interest

The authors declare that they have no known competing financial interests or personal relationships that could have appeared to influence the work reported in this paper.

Data availability

The data that has been used is confidential.

Acknowledgments

This work is supported by the National Natural Science Foundation of China under Grant No. 62071424, 62027805, and 62201499, Zhejiang Provincial Natural Science Foundation of China under Grant No. LD21F010002, Zhejiang Laboratory Foundation of China under Grant No. 2020KCDAB01 and State Key Laboratory of Reliability and Intelligence of Electrical Equipment No. EERI_KF2021013, Hebei University of Technology. S. Tan is supported by the start-up funds of Zhejiang University, the Zhejiang University/ Singapore University of Technology and Design (ZJU-SUTD) Innovation, Design and Entrepreneurship Alliance (IDEA) seed grant, and the Dynamic Research Enterprise for Multidisciplinary Engineering Sciences (DREMES) seed project of the Zhejiang University/ University of Illinois at Urbana-Champaign (ZJU-UIUC) joint research center.

References

- [1] W. Maass, Networks of spiking neurons: the third generation of neural network models, *Neural Netw.* 10 (9) (1997) 1659–1671.
- [2] J.P. Fernández, M.A. Vargas, J.M.V. García, J.A.C. Carrillo, J.J.C. Aguilar, A biological-like controller using improved spiking neural networks, *Neurocomputing* 463 (20) (2021) 237–250.
- [3] P.A. Merolla, et al., A million spiking-neuron integrated circuit with a scalable communication network and interface, *Science* 345 (6197) (2014) 668–673.
- [4] M. Davies, N. Srinivasa, T.-H. Lin, G. Chinya, Y. Cao, S.H. Choday, G. Dimou, P. Joshi, N. Imam, S. Jain, Y. Liao, C.-K. Lin, A. Lines, R. Liu, D. Mathaiikutty, S. McCoy, A. Paul, J. Tse, G. Venkataraman, Y.-H. Weng, A. Wild, Y. Yang, H. Wang, Loihi: A neuromorphic manycore processor with on-chip learning, *IEEE Micro* 38 (1) (2018) 82–99.
- [5] J. Kim, D. Kwon, S.Y. Woo, W. Kang, S. Lee, S. Oh, C. Kim, J. Bae, B. Park, J. Lee, Hardware-based spiking neural network architecture using simplified backpropagation algorithm and homeostasis functionality, *Neurocomputing* 428 (14) (2021) 153–165.
- [6] F. Ponulak, A. Kasinski, Supervised learning in spiking neural networks with ReSuMe: sequence learning, classification, and spike shifting, *Neural Comput.* 22 (2) (2010) 467–510.
- [7] J.H. Lee, T. Delbrück, M. Pfeiffer, Training deep spiking neural networks using backpropagation, *Front. Neurosci.* 10 (508) (2016) 1–13.

- [8] G. Orchard, C. Meyer, R. Etienne-Cummings, C. Posch, N. Thakor, R. Benosman, HFirst: a temporal approach to object recognition, *IEEE Trans. Pattern Anal. Mach. Intell.* No. 37 (10) (2015) 2028–2040.
- [9] H. Mostafa, Supervised learning based on temporal coding in spiking neural networks, *IEEE Trans. Neural Netw. Learn. Syst.* 29 (7) (2018) 3227–3235.
- [10] T. Masquelier, R. Guyonneau, S.J. Thorpe, Competitive STDP-based spike pattern learning, *Neural Comput.* 21 (5) (2009) 1259–1276.
- [11] P.U. Diehl, M. Cook, Unsupervised learning of digit recognition using spike-timing dependent plasticity, *Front. Comput. Neurosci.* 9 (99) (2015) 1–9.
- [12] C. Lammie, T. J. Hamilton, A. van Schaik, and M. Rahimi Azghadi, “Efficient FPGA Implementations of Pair and Triplet-Based STDP for Neuromorphic Architectures,” *IEEE Trans. Circuits Syst. I, Reg. Papers*, vol. 66, no. 4, pp. 1558–1570, April 2019.
- [13] M. Heidarpour, A. Ahmadi, M. Ahmadi, and M. Rahimi Azghadi, “CORDIC-SNN: On-FPGA STDP Learning with Izhikevich Neurons,” *IEEE Trans. Circuits Syst. I, Reg. Papers*, vol. 66, no. 7, pp. 2651–2661, July 2019.
- [14] D.B. Strukov, G.S. Snider, D.R. Stewart, R.S. Williams, The missing memristor found, *Nature* 453 (7191) (2008) 80–83.
- [15] S. Yu, Resistive random access memory (RRAM), *Synth. Lect. Emerg. Eng. Technol.* 2 (5) (Mar. 2016) 1–79.
- [16] W.-H. Chen, C. Dou, K.-X. Li, W.-Y. Lin, P.-Y. Li, J.-H. Huang, J.-H. Wang, W.-C. Wei, C.-X. Xue, Y.-C. Chiu, Y.-C. King, C.-J. Lin, R.-S. Liu, C.-C. Hsieh, K.-T. Tang, J.-J. Yang, M.-S. Ho, M.-F. Chang, CMOS-integrated memristive non-volatile computing-in-memory for AI edge processors, *Nature Electron.* 2 (9) (Sep. 2019) 420–428.
- [17] T. Tao et al., “Circuit Modeling for RRAM-Based Neuromorphic Chip Crossbar Array With and Without Write-Verify Scheme,” *IEEE Trans. Circuits Syst. I, Reg. Papers*, vol. 68, no. 5, pp. 1906–1916, May 2021.
- [18] V.A. Demin, D.V. Nekhaev, I.A. Surazhevsky, K.E. Nikiruy, A.V. Emelyanov, S. N. Nikolaev, V.V. Rylkov, M.V. Kovalchuk, Necessary conditions for STDP-based pattern recognition learning in a memristive spiking neural network, *Neural Netw.* 134 (Dec. 2021) 64–75.
- [19] A. Sboev, D. Vlasov, R. Rybka, Y. Davydov, A. Serenko, V. Demin, Modeling the Dynamics of Spiking Networks with Memristor-Based STDP to Solve Classification Tasks, *Mathematics* 9 (24) (2021) 3237.
- [20] Y. Huang, J. Liu, J. Harkin, L. McDaid, Y. Luo, An memristor-based synapse implementation using BCM learning rule, *Neurocomputing* 423 (Jan. 2021) 336–342.
- [21] M. Nouri, M. Jalilian, M. Hayati, D. Abbott, A Digital Neuromorphic Realization of Pair-Based and Triplet-Based Spike-Timing-Dependent Synaptic Plasticity, *IEEE Trans. Circuits Syst. II* 65 (6) (2018) 804–808.
- [22] T. Serrano-Gotarredona, T. Masquelier, T. Prodromakis, G. Indiveri, B. Linares-Barranco, STDP and STDP variations with memristors for spiking neuromorphic learning systems, *Front. Neurosci.* 7 (2) (2013) 1–16.
- [23] S. Bianchi, G. Pedretti, I. Muñoz-Martín, A. Calderoni, N. Ramaswamy, S. Ambrogio, D. Ielmini, A Compact Model for Stochastic Spike-Timing-Dependent Plasticity (STDP) Based on Resistive Switching Memory (RRAM) Synapses, *IEEE Trans. on Electron Devices* 67 (7) (2020) 2800–2806.
- [24] D. Querlioz, O. Bichler, P. Dollfus, C. Gamrat, Immunity to Device Variations in a Spiking Neural Network with Memristive Nanodevices, *IEEE Trans. Nanotechnol.* 12 (3) (May 2013) 288–295.
- [25] X. Wu, V. Saxena, K. Zhu, S. Balagopal, A CMOS Spiking Neuron for Brain-Inspired Neural Networks With Resistive Synapses and In Situ Learning, *IEEE Trans. Circuits Syst., II, Exp. Briefs, Nov.* 62 (11) (2015) 1088–1092.
- [26] Y. Lecun, L. Bottou, Y. Bengio, P. Haffner, Gradient-based learning applied to document recognition, *Proc. IEEE* 86 (11) (Nov. 1998) 2278–2324.
- [27] B. Romain, and G. Dan. *The Brian Spiking Neural Network Simulator*. Accessed: Apr. 4, 2019. [Online]. Available: <http://briansimulator.org>.
- [28] Z. Zhao, L. Qu, L. Wang, Q. Deng, N. Li, Z. Kang, S. Guo, W. Xu, A Memristor-Based Spiking Neural Network With High Scalability and Learning Efficiency, *IEEE Trans. Circuits Syst. II* 67 (5) (2020) 931–935.
- [29] M. Hansen, F. Zahari, M. Ziegler, H. Kohlstedt, Double-Barrier Memristive Devices for Unsupervised Learning and Pattern Recognition, *Front. Neurosci.* 11 (91) (2017) 1–11.
- [30] Y. Guo, H. Wu, B. Gao, H. Qian, Unsupervised Learning on Resistive Memory Array Based Spiking Neural Networks, *Front. Neurosci.* 13 (812) (Aug. 2019) 1–16.
- [31] C. Zamarreño-Ramos, L.A. Camuñas-Mesa, J.A. Pérez-Carrasco, T. Masquelier, T. Serrano-Gotarredona, B. Linares-Barranco, On spike-timing-dependent-plasticity, memristive devices, and building a self-learning visual cortex, *Front. Neurosci.* 5 (5) (March 2011) 1–22.
- [32] MATLAB, Release R2017a, MathWorks, Natick, MA, USA, 2017.



Tuomin Tao received the B.S. degree in engineering from Zhejiang University, Hangzhou, China, in 2018, where she is currently pursuing the Ph.D. degree with the College of Information Science and Electronics Engineering, Zhejiang University–University of Illinois at Urbana–Champaign Institute. Her current research interests include signal integrity analysis for neuromorphic chip and machine learning techniques for EMI analysis of advanced package.



Da Li received the B.S. degree in 2014, and the Ph.D. degree in 2019, from Zhejiang University, Hangzhou, China, both in electrical engineering. From 2017 to 2018, he worked at Nanyang Technological University, Singapore, as a Project Researcher. From 2019 to 2021, he joined Science and Technology on Antenna and Microwave Laboratory, Nanjing, China, as a Research Fellow. He is currently an assistant professor at Zhejiang University. His research interests include machine learning, antennas, metasurfaces, and electromagnetic compatibility. Dr. Li has authored or coauthored more than 30 refereed papers and served as Reviewers for 6 technical journals and TPC Members of 2 IEEE conferences.



Hanzhi Ma received the B.S. degree and Ph.D. degree in electrical engineering from Zhejiang University, Hangzhou, China, in 2017 and 2022. She is currently an assistant professor at Zhejiang University. Her research interests include machine learning techniques for EMI/SI/PI analysis and signal integrity analysis for neuromorphic chip. She has authored or coauthored more than 30 technical papers and served as Reviewers for 5 technical journals and TPC Members of 6 IEEE conferences. She received the President’s Memorial Award from IEEE Electromagnetic Compatibility Society in 2020 and 2021, and the Best student paper from Asia-Pacific International Symposium on Electromagnetic Compatibility in 2022.



Yan Li (S’17–M’19–SM’21) received the Ph.D. degree in electrical engineering from Hebei University of Technology, Tianjin, China, in 2019. From 2016 to 2019, she carried out her PhD research at Zhejiang University under the joint PhD program. In Sept 2019, she joined China Jiliang University where she is currently Assistant Professor at the College of Information Engineering, China Jiliang University, Hangzhou, China. Her current research interests include signal integrity and power integrity of 3-D integrated circuit, fast and efficient computational electromagnetics, electromagnetic modeling and experimental method and its application in high-speed electronics.

Dr. Li received an Outstanding Young Scientist Award at the Joint IEEE International Symposium on Electromagnetic Compatibility & Asia-Pacific Symposium on Electromagnetic Compatibility, Singapore (2018), a Best Student Paper Award at the IEEE International Symposium on Electromagnetic Compatibility, Xi'an, China (2017), an Outstanding Doctoral Graduate Award of Hebei Province (2019), and Excellent Doctoral Dissertation Award of Hebei University of Technology (2020). She was the Secretary Chair and Section Chair of The International Workshops on Electromagnetic Compatibility of Integrated Circuits (EMC COMPO), Haining, China (2019), Section Chair of IEEE MTT-S International Conference on Numerical Electromagnetic and Multiphysics Modeling and Optimization (IEEE MTT-S NEMO), Hangzhou China (2020), and Section Chair of the 13th Global Symposium on Millimeter Waves & Terahertz (GSMM), Nanjing, China (2021).



Shurun Tan received the B.E. degree in information engineering and M.Sc. degree in electromagnetic field and microwave techniques from the Southeast University, Nanjing, China, in 2009 and 2012, respectively, and the Ph.D. degree in electrical engineering from the University of Michigan, Ann Arbor, MI, USA, in Dec. 2016.

Dr. Tan is an assistant professor in the Zhejiang University / University of Illinois at Urbana-Champaign Institute located at the International Campus of Zhejiang University, Haining, China. He is also affiliated with the State Key Laboratory of Modern Optical Instrumentation, College of Information Science and Electronic Engineering, Zhejiang University, Hangzhou, China. He is also an adjunct assistant professor in the Department of Electrical and Computer Engineering, University of Illinois at Urbana-Champaign, Urbana, USA. From Dec. 2010 to Nov. 2011, he was a Visiting Student with the Department of Electrical and Computer Engineering, the University of Houston, Houston, TX, USA. From Sep. 2012 to Dec. 2014, he was a PhD candidate with the Department of Electrical Engineering, the University of Washington, Seattle, WA, USA. From Jan. 2015 to Dec. 2018, he had been affiliated with the Radiation Laboratory, and the Department of Electrical Engineering and Computer Science, the University of Michigan, Ann Arbor, first as a PhD candidate, and then as a postdoctoral research fellow since Jan. 2017.

He is working on electromagnetic theory, computational and applied electromagnetics. His research interests include microwave remote sensing of environment, complex EM environment effects, neuromorphic chip heterogeneous integration, electromagnetic basis for bio-signaling, nanostructure scattering and characterization, etc. He is especially interested in electromagnetic multiple scattering theory for wave propagation and scattering in random media, periodic structures and cavities.



En-Xiao Liu received the bachelor (96) and master (99) degrees from the Xi'an Jiaotong University, and the PhD (05) degree in electrical engineering from the National University of Singapore (NUS).

From 1999 to 2001, Dr. Liu was with North China Electric Power Design Institute, Beijing, China. In 2005 he joined the Institute of High Performance Computing (IHPC), A*STAR, Singapore, where he is currently Senior Scientist and Deputy Department Director of the Electronics and Photonics Department. He is also an adjunct Associate Professor at the Electrical and Computer Engineering of NUS. He has published more than 100 papers and three book chapters. His research interests are in the areas of computational electromagnetics, high-speed electronics, and electromagnetic compatibility (EMC).

Dr. Liu received Singapore President's Technology Award (2019), the ASEAN Outstanding Engineering Achievement Award and IES Prestigious Engineering Achievement Award (2019), the IEEE EMC Society Technical Achievement Award (2016), Best Paper and Best Industry Project Awards, and other awards. He was an IEEE EMC Society Distinguished Lecturer. Presently he is Associate Editor of two IEEE Transactions (EMC and CPMT). He has been serving the IEEE EMC Singapore Chapter as Chair and executive committee member, and contributing regularly to various international conferences in different capacities, such as Organizing Chair, Technical Program Chair, International Advisory/Steering Committee member, and General Chair.



Jose Schutt-Aine received the B.S. degree in electrical engineering from the Massachusetts Institute of Technology, Cambridge, MA, USA, in 1981, and the M.S. and Ph.D. degrees from the University of Illinois at Urbana-Champaign (UIUC), Urbana, IL, USA, in 1984 and 1988, respectively.

From 1981 to 1983, he was with the Hewlett Packard Technology Center, Santa Rosa, CA, USA, as an Application Engineer, where he was involved in research on microwave transistors and high-frequency circuits. In 1988, he joined the Electrical and Computer Engineering Department, UIUC, as a member of the Electromagnetics and Coordinated Science Laboratories, where he is currently involved in research on signal integrity for high-speed digital and high-frequency applications. He is a consultant for several corporations. His current research interests include the study of signal integrity and the generation of computer-aided design tools for high-speed digital systems.

Dr. Schutt-Aine was a recipient of several research awards, including the 1991 National Science Foundation MRI Award, the National Aeronautics and Space Administration Faculty Award for Research, in 1992, the NSF MCAA Award, in 1996, and the UIUC-National Center for Superconducting Applications Faculty Fellow Award, in 2000.



Er-Ping Li is currently a Changjiang-Distinguished Professor, Department of Information Science and Electronic Engineering, Zhejiang University, China; Dean of Joint Institute of Zhejiang University- University of Illinois at Urbana-Champaign. Since 1989, he has served as a Research Fellow, Principal Research Engineer, Associate Professor and the Technical Director at the Singapore Research Institute and University. In 2000, he joined the Singapore A*STAR Research Institute of High Performance Computing as a Principal Scientist and Director. Dr. Li authored or co-authored over 300 papers published in the referred international journals, authored two books published by John-Wiley-IEEE Press and Cambridge University Press. He holds and has filed a number of patents at the US patent office. His research interests include electrical modeling and design of micro/nano-scale integrated circuits, 3D electronic package integration and nano-plasmonic technology.

Dr. Li is a Fellow of IEEE, and a Fellow of MIT Electromagnetics Academy, USA. He is the recipient of 2015 IEEE Richard Stoddard Award on EMC, IEEE EMC Technical Achievement Award, Singapore IES Prestigious Engineering Achievement Award, and Changjiang Chair Professorship Award from the Ministry of Education in China, and number of Best Paper Awards. He was elected to the IEEE EMC Distinguished Lecturer in 2007. He served as an Associate Editor for the IEEE MICROWAVE AND WIRELESS COMPONENTS LETTERS from 2006-2008 and served Guest Editor for 2006 and 2010 IEEE TRANSACTIONS on EMC Special Issues, Guest Editor for 2010 IEEE TRANSACTIONS on MTT APMC Special Issue. He is currently an Associate Editor for the IEEE TRANSACTIONS ON EMC and IEEE TRANSACTIONS on CPMT. He is the Founding Member of IEEE MTT-RF Nanotechnology Committee. He has been a General Chair and Technical Chair, for many international conferences. He was the President for 2006 International Zurich Symposium on EMC, the Founding General Chair for Asia-Pacific EMC Symposium, General Chair for 2008, 2010, 2012, 2016 APEMC, and 2010 IEEE Symposium on Electrical Design for Advanced Packaging Systems . He has been invited to give numerous invited talks and plenary speeches at various international conferences and forums.